

## Supporting Information

# Structure induced activity enhancement of tungsten oxide for tetrabromobisphenol A photodegradation under visible light illumination

Shiman Zhou, Qianqian Zhu\*, Denan Li, Lifeng Zhang, Yanshuo Li\*, Zhenxin Zhang\*

<sup>a</sup> School of Materials Science and Chemical Engineering, Ningbo University, Ningbo 315211, China

<sup>b</sup> Zhejiang Hymater New Materials Co., Ltd. Ningbo, Zhejiang, 315034, P. R. China

\*Corresponding Author. E-mail: zhuqianqian@nbu.edu.cn (Q.Z.); E-mail: liyanshuo@nbu.edu.cn (Y.L.); E-mail: zhangzhenxin@nbu.edu.cn (Z.Z.)

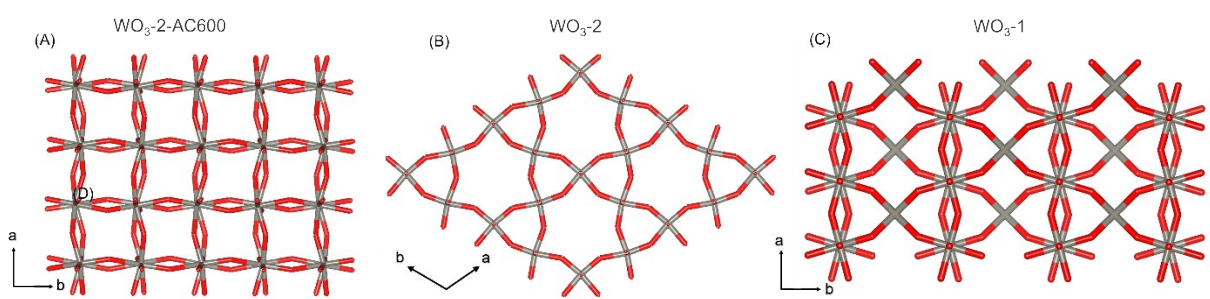


**Fig. S1**  $\text{WO}_3$  with different crystalline phases, (A) monoclinic, (B) hexagonal, and (C) orthorhombic, W (gray), O (red).

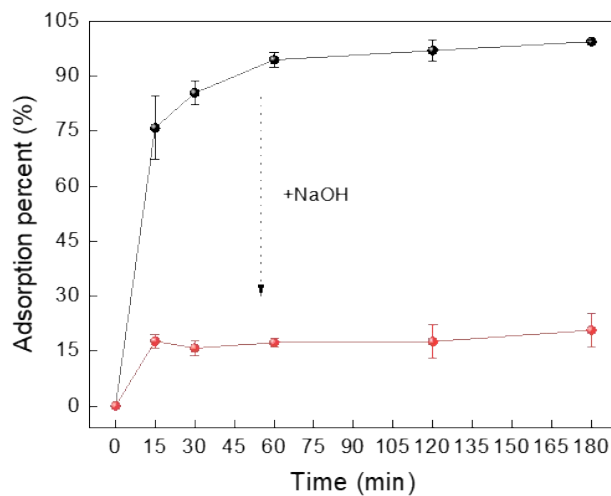


**Fig. S2** (black) Adsorption of TBBPA on  $\text{WO}_3$ -2-AC600 under dark at room temperature and (red) after adding NaOH solution. Adsorption conditions:  $[\text{TBBPA}]_0 = 50.0 \mu\text{mol/L}$ ,  $[\text{WO}_3]_0 = 0.5 \text{ g/L}$ ,  $[\text{NaOH}] = 10.0 \text{ mmol/L}$  and 0.02 mol/L buffer ( $\text{Na}_2\text{HPO}_4$ - $\text{NaH}_2\text{PO}_4$  at pH 8.2).

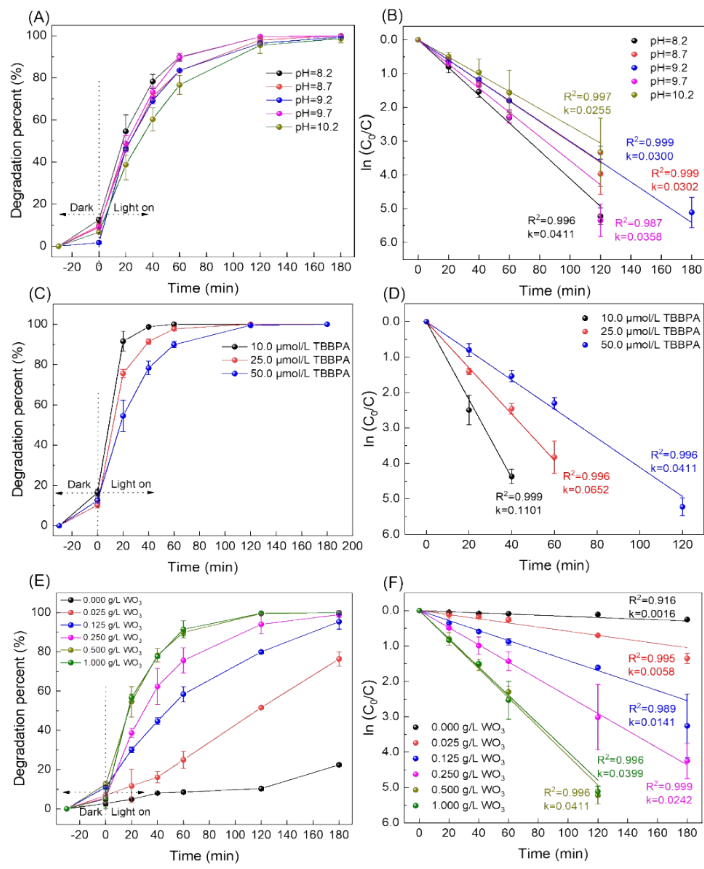


**Fig. S3** (A) Effect of initial pH on the TBBPA photodegradation and (B) pseudo-first order kinetic curves, reaction conditions:  $[\text{TBBPA}]_0 = 50.0 \mu\text{mol/L}$ ,  $[\text{H}_2\text{O}_2]_0 = 1.25 \text{ mmol/L}$ ,  $[\text{WO}_3]_0 = 0.500 \text{ g/L}$ , and 0.02 mol/L buffer ( $\text{Na}_2\text{HPO}_4\text{-NaH}_2\text{PO}_4$  at pH 8.2-8.7,  $\text{Na}_2\text{CO}_3\text{-NaHCO}_3$  at pH 9.2-10.2). (C) Effect of TBBPA concentration on the TBBPA photodegradation and (D) pseudo-first order kinetic curves, reaction conditions:  $[\text{TBBPA}]_0 = 10.0\text{-}50.0 \mu\text{mol/L}$ ,  $[\text{H}_2\text{O}_2]_0 = 1.25 \text{ mmol/L}$ ,  $[\text{WO}_3]_0 = 0.500 \text{ g/L}$ , and 0.02 mol/L buffer ( $\text{Na}_2\text{HPO}_4\text{-NaH}_2\text{PO}_4$  at pH 8.2). (E) Effect of the amount of  $\text{WO}_3\text{-2-AC600}$  on the TBBPA photodegradation and (F) pseudo-first order kinetic curves, reaction conditions:  $[\text{TBBPA}]_0 = 50.0 \mu\text{mol/L}$ ,  $[\text{H}_2\text{O}_2]_0 = 1.25 \text{ mmol/L}$ ,  $[\text{WO}_3]_0 = 0.000\text{-}1.000 \text{ g/L}$ , and 0.02 mol/L buffer ( $\text{Na}_2\text{HPO}_4\text{-NaH}_2\text{PO}_4$  at pH 8.2).

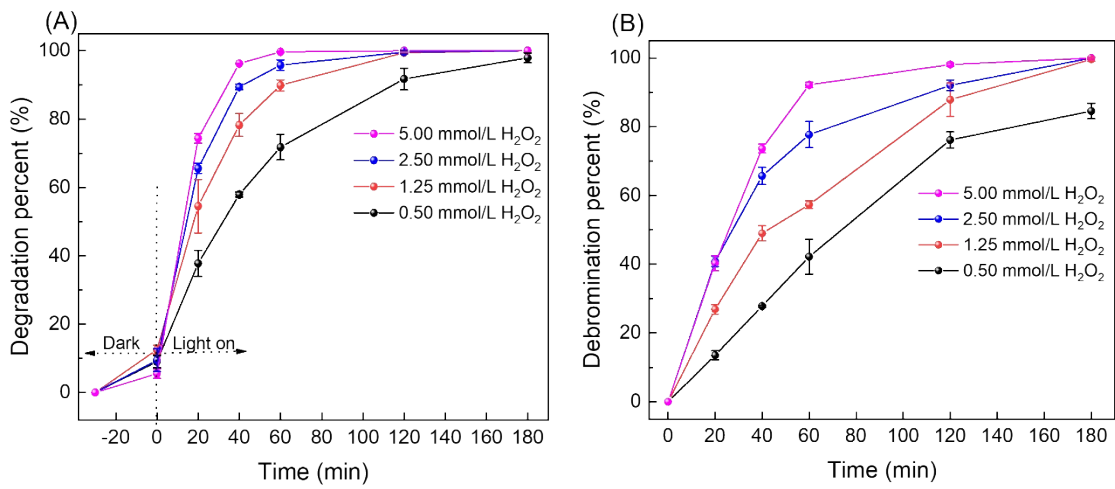


**Fig. S4** (A) Degradation percent and (B) debromination percent of TBBPA in different concentrations of  $\text{H}_2\text{O}_2$ , reaction conditions:  $[\text{TBBPA}]_0 = 50.0 \mu\text{mol/L}$ ,  $[\text{WO}_3]_0 = 0.500 \text{ g/L}$ , and  $0.02 \text{ mol/L}$  buffer ( $\text{Na}_2\text{HPO}_4\text{-NaH}_2\text{PO}_4$  at pH 8.2).

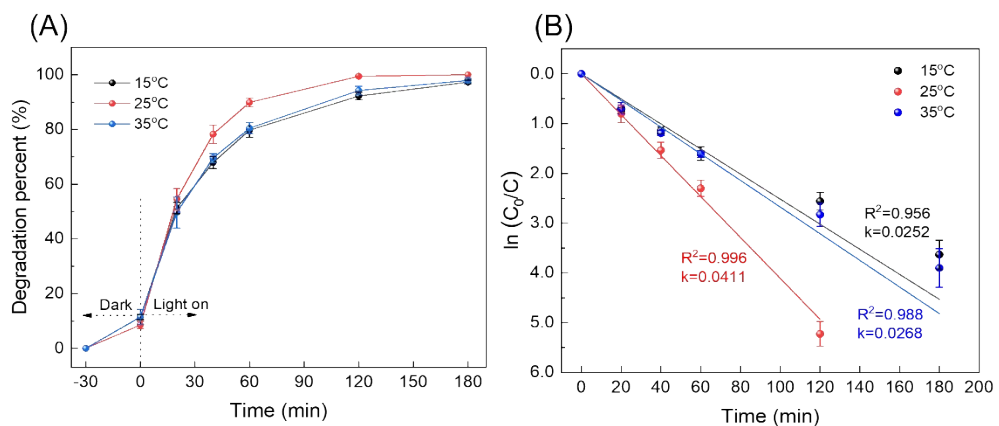


**Fig. S5** Degradation percent of TBBPA at different temperatures, reaction conditions:  $[TBBPA]_0 = 50.0 \mu\text{mol/L}$ ,  $[\text{H}_2\text{O}_2]_0 = 1.25 \text{ mmol/L}$ ,  $[\text{WO}_3]_0 = 0.5 \text{ g/L}$ , and  $0.02 \text{ mol/L}$  buffer ( $\text{Na}_2\text{HPO}_4$ - $\text{NaH}_2\text{PO}_4$  at pH 8.2).

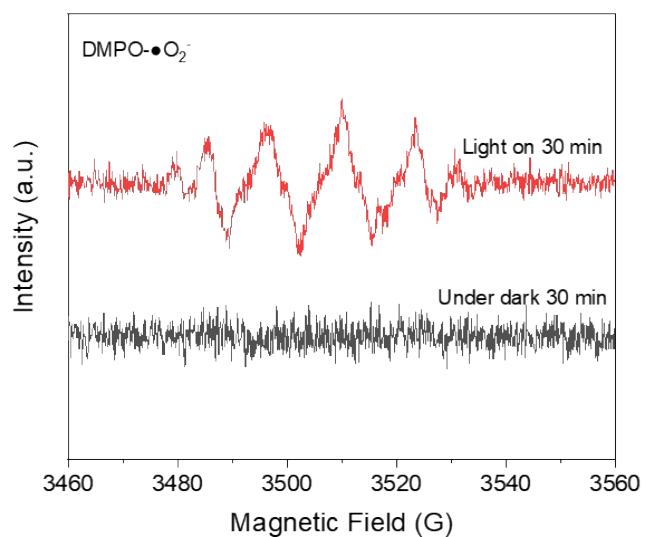


**Fig. S6** ESR profiles of TBBPA degradation using only O<sub>2</sub> without peroxides using DMPO as radical capturer •O<sub>2</sub><sup>-</sup> in methanol.

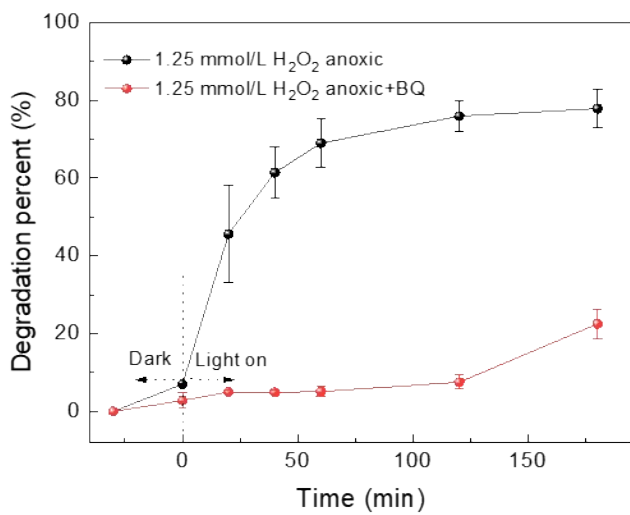


**Fig. S7** The degradation percent of TBBPA without air when BQ was added or not, reaction conditions:  $[TBBPA]_0 = 50.0 \mu\text{mol/L}$ ,  $[H_2O_2]_0 = 1.25 \text{ mmol/L}$ ,  $[BQ]_0 = 10.0 \text{ mmol/L}$ ,  $[WO_3]_0 = 0.500 \text{ g/L}$ , and 0.02 mol/L buffer ( $\text{Na}_2\text{HPO}_4$ - $\text{NaH}_2\text{PO}_4$  at pH 8.2).

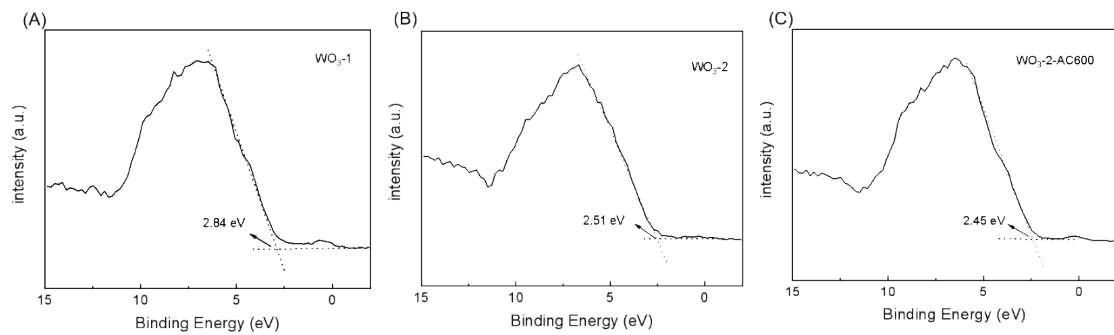


**Fig. S8** VB-XPS profiles of (A)  $\text{WO}_3\text{-}1$ , (B)  $\text{WO}_3\text{-}2$ , and (C)  $\text{WO}_3\text{-}2\text{-AC600}$

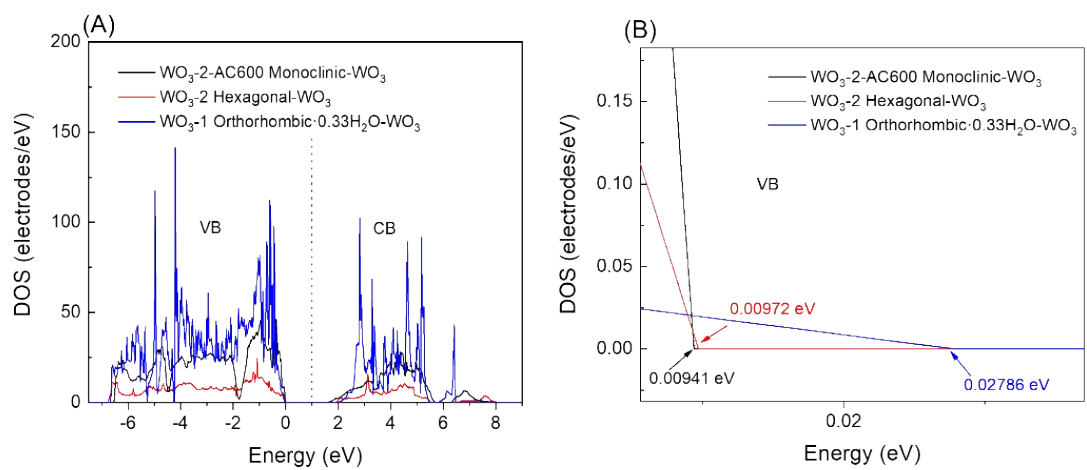


**Fig. S9** (A) DOS profiles of WO<sub>3</sub> with different crystalline structures and (B) enlarged DOS profiles.

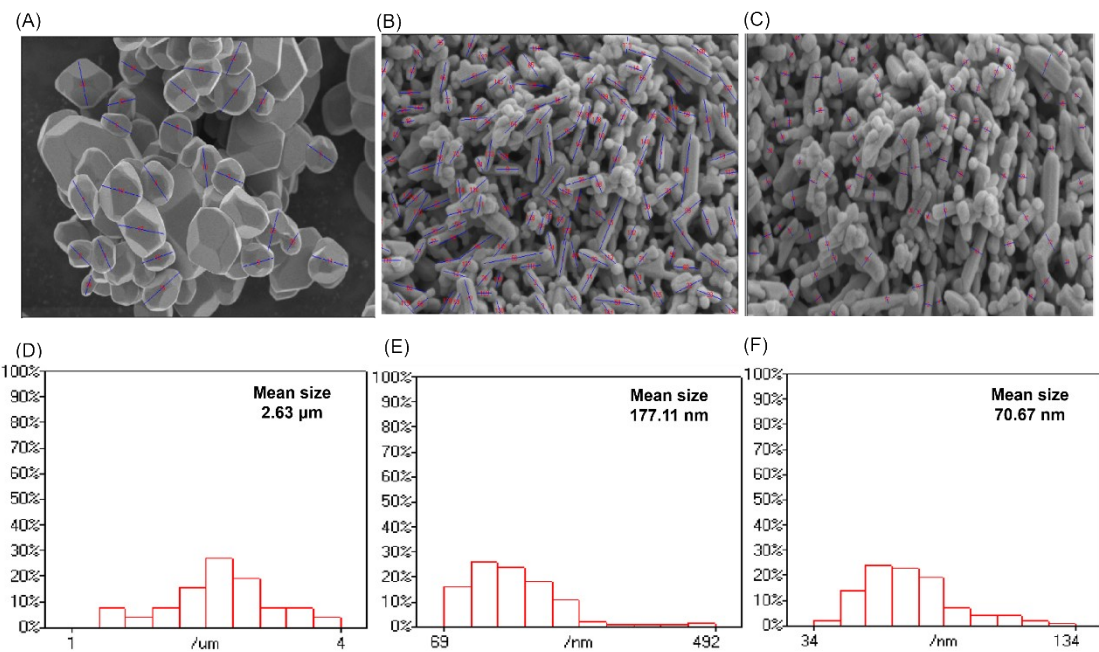


**Fig. S10** SEM images of (A) WO<sub>3</sub>-2-AC900 with selected diameters, (B) WO<sub>3</sub>-2-AC600 with selected length, (C) WO<sub>3</sub>-2-AC600 with selected diameter, particle size distribution of (D) WO<sub>3</sub>-2-AC900, (E) length distribution of WO<sub>3</sub>-2-AC600, and (F) diameter distribution of WO<sub>3</sub>-2-AC600.

The method for estimating surface area of different monoclinic WO<sub>3</sub>

According to SEM images, WO<sub>3</sub>-2-AC600 was nanorod with different scales in diameter and length and WO<sub>3</sub>-2-AC900 was polyhedral with similar scales in each diameter. WO<sub>3</sub>-2-AC900 was regarded as a sphere, and the surface area was calculated based on  $S_1 = 4\pi(r_1)^2/(4/3)\pi(r_1)^3\rho$ , where  $S_1$  was catalyst surface area per unit mass of WO<sub>3</sub>-2-AC900,  $r_1$  was radius, and  $\rho$  was density of WO<sub>3</sub>-2-AC900. Furthermore, WO<sub>3</sub>-2-AC600 was regarded as a cylinder, using the surface area calculation formula  $S_2 = 2\pi r_2(r_2+h)/(\pi(r_2)^2 h \rho)$  of the cylinder, where  $S_2$  was catalyst surface area per unit mass of WO<sub>3</sub>-2-AC600,  $r_2$  was the radius of the cylinder, and  $h$  was the height of the cylinder.  $S_2/S_1=2r_1(r_2+h)/3r_2h$ . When  $r_1 = 1.315 \mu\text{m}$ ,  $r_2 = 35.335 \text{ nm}$ , and  $h = 177.11 \text{ nm}$ ,  $S_1/S_2 = 29.76$ . Therefore, the surface area of WO<sub>3</sub>-2-AC600 was estimated to be 29.76 times as high as that of WO<sub>3</sub>-2-AC900.

Therefore, the dose of WO<sub>3</sub>-2-AC900 was 40 times as high as the dose of WO<sub>3</sub>-2-AC600 to ensure the surface area of the catalysts to be close for comparison. When the concentration of WO<sub>3</sub>-2-AC900 reached 1.000 g/L (Fig. S9), the degradation percent was about 70.3% after 180 min, and the degradation effect was still lower than that of 0.025 g/L WO<sub>3</sub>-2-AC600 (76.4%) (Fig. S2E).

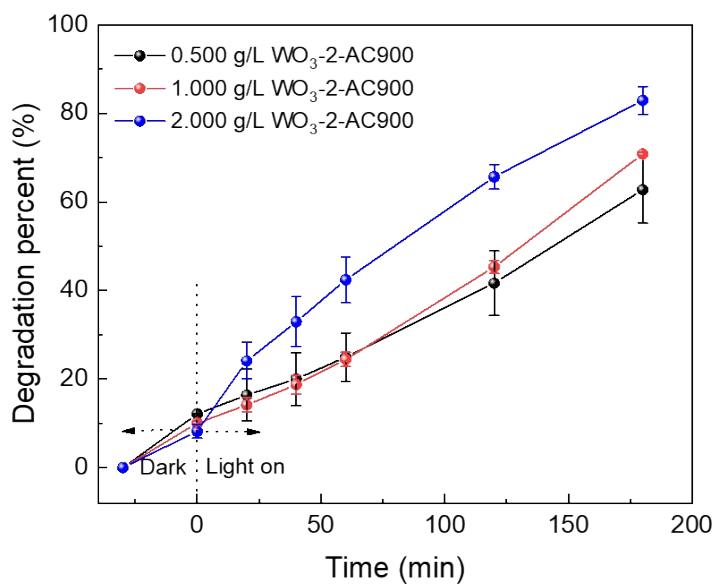


**Fig. S11** Effect of the amount of  $\text{WO}_3\text{-2-AC900}$  on the TBBPA photodegradation, reaction conditions:  $[\text{TBBPA}]_0 = 50.0 \mu\text{mol/L}$ ,  $[\text{H}_2\text{O}_2]_0 = 1.25 \text{ mmol/L}$ ,  $[\text{WO}_3]_0 = 0.500\text{-}2.000 \text{ g/L}$ , and  $0.02 \text{ mol/L}$  buffer ( $\text{Na}_2\text{HPO}_4\text{-NaH}_2\text{PO}_4$  at pH 8.2).

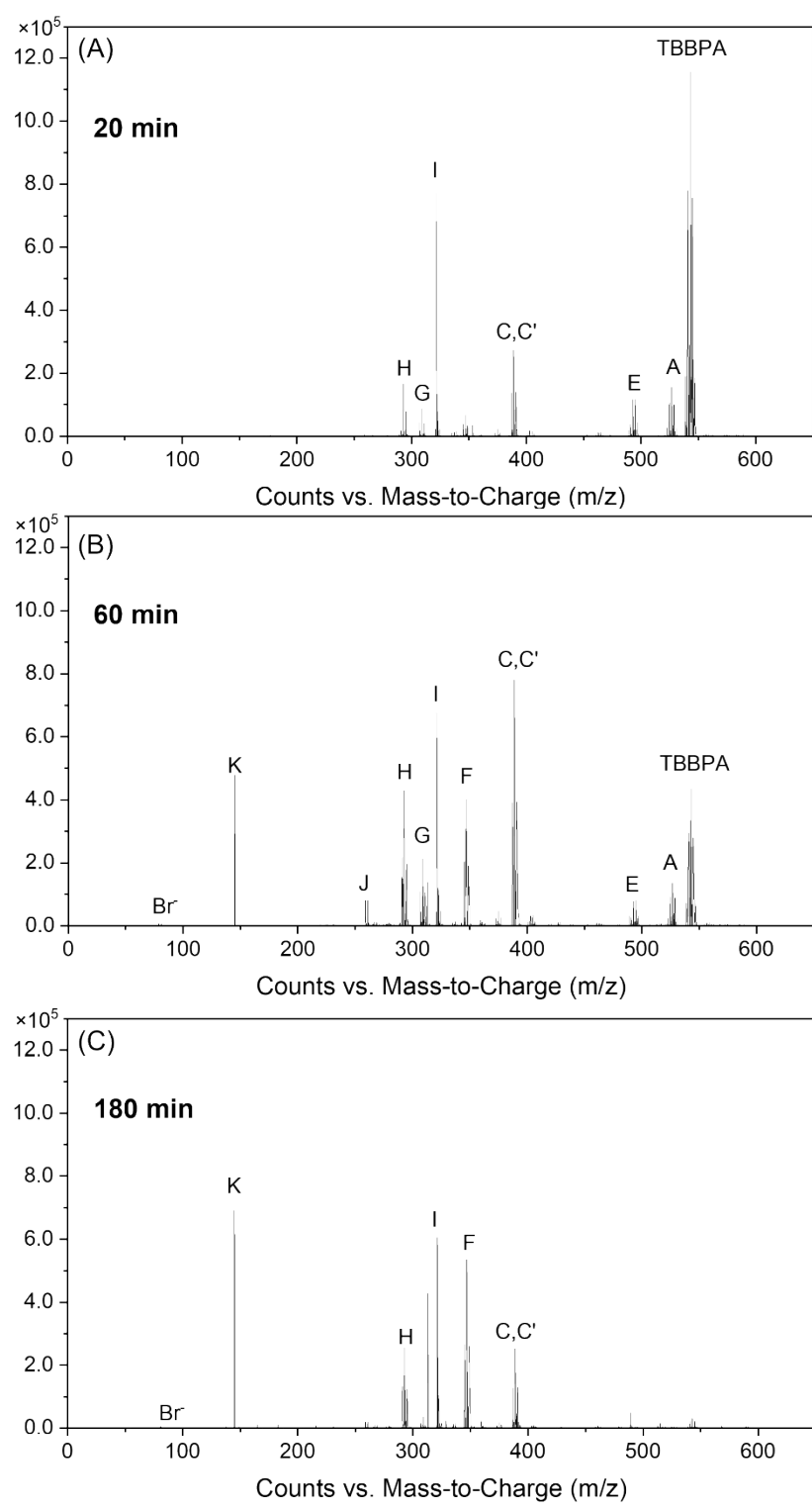


**Fig. S12** The HRMS profiles of the TBBPA degradation at (A) 20 min, (B) 60 min, and (C) 180 min.

**Table S1.** Results of the characterization of various  $\text{WO}_3$  obtained by a hydrothermal method.

Catalyst	Crystalline phase	BET Surface area ( $\text{m}^2/\text{g}$ )	Bandgap energy (eV)
$\text{WO}_3\text{-1}$	Orthorhombic	6.1	2.73
$\text{WO}_3\text{-1-AC600}$	Monoclinic	1.0	2.56
$\text{WO}_3\text{-2}$	Hexagonal	46.3	2.66
$\text{WO}_3\text{-2-AC400}$	Hexagonal	22.1	2.68
$\text{WO}_3\text{-2-AC600}$	Monoclinic	9.8	2.65
$\text{WO}_3\text{-2-AC900}$	Monoclinic	<1.0	2.53

**Table S2.** Comparisons of TBBPA degradation between the prepared composite and some previously reported catalysts.

Catalyst	Dosage	Light source	TBBPA concentration ( $\mu\text{mol/L}$ )	Time	Efficiency (%)	Debromination percent	Peroxide (mmol/L)	References
	(g/L)							
WO <sub>3</sub> -1-AC600	0.5	300 W xenon lamp	50.0	180 min	100.0	100.0	H <sub>2</sub> O <sub>2</sub>	This work
Fe <sub>3-x</sub> Ti <sub>x</sub> O <sub>4</sub>	0.125	6 W UV-light tube	36.8	180 min	92.1	-	H <sub>2</sub> O <sub>2</sub>	<sup>1</sup> (10.0)
TiO <sub>2</sub>	0.2	100 W high-pressure mercury lamp	91.9	120 min	98.8	-	KPS (2.0)	<sup>2</sup>
Alkaline TiO <sub>2</sub>	0.25	75 W high-pressure Hg lamp (UV)	41.7	120 min	100.0	100.0	-	<sup>3</sup>
MoS <sub>2</sub> /SnIn <sub>4</sub> S <sub>8</sub>	0.5	300 W xenon lamp	18.4	180 min	89.1	50.0	-	<sup>4</sup>
ZnTMPyP	5.0	16 W LED lamps	50.0	180 min	84.0	32.0	-	<sup>5</sup>
Graphene-TiO <sub>2</sub>	0.25	230 W Hg lamp	18.4	60 min	95.5	-	-	<sup>6</sup>
CuO/Ce <sub>2</sub> O <sub>3</sub>	0.5	500 W Xenon lamp	9.2	120 min	80.46	-	-	<sup>7</sup>
F-TiO <sub>2</sub> -g-C <sub>3</sub> N <sub>4</sub>	0.5	300 W Xenon lamp	18.4	120 min	95.0	-	-	<sup>8</sup>
BiOBr	0.5	800 W xenon lamp	1.84	60 min	100.0	-	-	<sup>9</sup>
tourmaline-TiO <sub>2</sub>	1.0	500W medium pressure mercury lamp	18.4	60 min	100.0	-	-	<sup>10</sup>
MIP@C-Fe-Nx	0.5	-	18.4	90 min	100.0	-	PS (1.26)	<sup>11</sup>
CuFe <sub>2</sub> O <sub>4</sub>	0.1	-	18.4	180 min	100.0	67.0	PMS (1.5)	<sup>12</sup>
nZVI	3.0	-	9.2	12 h	78.32	-	PS (25.0)	<sup>13</sup>

FeTPPS	5.0	-	50.0	30 min	95.0	0	PMS	<sup>14</sup>
		μmol/L					(0.125)	
Fe <sub>3</sub> O <sub>4</sub> /MWCNT	0.5	-	18.4	180 min	90.2	-	H <sub>2</sub> O <sub>2</sub> (0.1)	<sup>15</sup>
Fe <sup>3+</sup> /S <sub>2</sub> O <sub>4</sub> <sup>2-</sup>	200.0	-	1.0	60 min	93.8	83.9	PS (0.2)	<sup>16</sup>

KPS: K<sub>2</sub>S<sub>2</sub>O<sub>8</sub>; PMS: KHSO<sub>5</sub>; PS: S<sub>2</sub>O<sub>4</sub><sup>2-</sup>

**Table S3.** Toxicity evaluation of Intermediate to Fathead minnow.

Intermediate	Chemical structure	LC50 (mg/L) For Fathead minnow
TBBPA		0.045
A		0.0452
B		0.18
B'		0.18
C		0.13
C'		0.19
D		0.10
E		0.13
G		3.5
H		1.61
J		N/A

K		N/A
---	--	-----

**Reference:**

- 1 Y. Zhong, X. Liang, Y. Zhong, J. Zhu, S. Zhu, P. Yuan, H. He and J. Zhang, *Water Res.*, 2012, **46**, 4633–4644.
- 2 Q. Li, L. Wang, L. Zhang and H. Xie, *Res. Chem. Intermed.*, 2019, **45**, 757–768.
- 3 S. Horikoshi, T. Miura, M. Kajitani, N. Horikoshi and N. Serpone, *Appl. Catal. B Environ.*, 2008, **84**, 797–802.
- 4 R. Weng, F. Tian, Z. Yu, J. Ma, Y. Lv and B. Xi, *Chemosphere*, 2021, **285**, 131542.
- 5 Q. Zhu, M. Igarashi, M. Sasaki, T. Miyamoto, R. Kodama and M. Fukushima, *Appl. Catal. B Environ.*, 2016, **183**, 61–68.
- 6 M. Cao, P. Wang, Y. Ao, C. Wang, J. Hou and J. Qian, *Chem. Eng. J.*, 2015, **264**, 113–124.
- 7 A. Zhu, P. Liu, Z. Wang, Z. Liu, A. Liu and L. Guan, *J. Environ. Chem. Eng.*, 2022, **10**, 108878.
- 8 P. Chen, S. Di, X. Qiu and S. Zhu, *Appl. Surf. Sci.*, 2022, **587**, 152889.
- 9 J. Xu, W. Meng, Y. Zhang, L. Li and C. Guo, *Appl. Catal. B Environ.*, 2011, **107**, 355–362.
- 10 N. Li, J. Zhang, C. Wang and H. Sun, *J. Mater. Sci.*, 2017, **52**, 6937–6949.
- 11 C. Zeng, Y. Wang, T. Xiao, Z. Yan, J. Wan and Q. Xie, *J. Hazard. Mater.*, 2022, **424**, 127499.
- 12 Y. Ding, L. Zhu, N. Wang and H. Tang, *Appl. Catal. B Environ.*, 2013, **129**, 153–162.
- 13 X. Yuan, T. Li, Y. He and N. Xue, *Chemosphere*, 2021, **284**, 131166.
- 14 Q. Zhu, Y. Mizutani, S. Maeno and M. Fukushima, *Molecules*, 2013, **18**, 5360–5372.
- 15 L. Zhou, H. Zhang, L. Ji, Y. Shao and Y. Li, *RSC Adv.*, 2014, **4**, 24900.
- 16 W. Song, M. Li, S. Xu, Z. Wang, J. Li, X. Zhang, W. Qiu, Z. Wang, Q. Song, K. Bhatt and C. Fu, *Environ. Pollut.*, 2023, **316**, 120579.